

The Razor: A 3D Printed UAV

A Thesis Presented to
the Faculty of the School of Engineering and Applied Science
University of Virginia

in partial fulfillment of the requirements for the degree
Master of Science (Mechanical and Aerospace Engineering)

by
Aaron L. Lam

May 2015

APPROVAL SHEET

The thesis
is submitted in partial fulfillment of the requirements
for the degree of
Master of Science

Aaron L Lam

AUTHOR

The thesis has been read and approved by the examining committee:

Hossein Haj-Hariri

Advisor

James C. McDaniel

Christopher Goyne

George L. Cahen

David A. Sheffler

Accepted for the School of Engineering and Applied Science:

James H. Ayl

Dean, School of Engineering and Applied Science

May
2015

Abstract

In the following paper, the process of identifying benefits and problems of 3D printing with respect to small, autonomous aircraft is detailed. This serves as a proof-of-concept that such an UAV can be fabricated with minimal requirements on skill and labor in small labs equipped with 3D printers, as well as the option of rapid incorporation of modifications to the airframe. The problems introduced by 3D printing are the relatively heavy airframes required by the materials, large tolerances involved, and an inherent internal weakness in one direction of every part. Nevertheless, the design presented has been proven to have stable and controllable flight characteristics and a very short assembly process. It has already undergone substantial iteration based on both empirical data from flight testing and from simulation software. This has resulted in an aircraft that can be launched by multiple methods, is optimized for a low speed loiter mission, and has a significant amount of damage tolerance and payload.

Table of Contents

Abstract.....	2
Table of Contents.....	3
Table of Figures.....	4
1. Introduction.....	5
1.1. Project Background.....	5
1.2. Problem Statement.....	5
2. 3D Printing.....	6
2.1. Constraints.....	6
2.1.1. Fortus 400MC Large.....	6
2.1.2. Materials.....	7
2.1.3. Part Orientation Due to Grains and Airfoil.....	7
2.2. S3D.....	8
2.2.1. Support Material.....	8
2.2.2. Part Orientation due to S3D.....	8
2.2.3. Break Away Sections.....	9
2.3. Printing Problems.....	9
2.3.1. Warping of Parts.....	9
2.3.2. Removing Components from Tray and Attachment Sizes.....	10
2.3.3. Unexplained Printing Errors.....	11
3. Technical Aspects of the Design.....	11
3.1. Aerodynamics/Sizing.....	11
3.1.1. Initial Simulation.....	12
3.1.2. RealFlight 6.5 Optimized.....	13
3.2. Weight and Balance.....	15
3.2.1. Components and Placement.....	15
3.2.2. Tray Design.....	16
3.2.3. Payload Placement.....	16
3.3. Propulsion.....	16
3.4. Structure.....	17
3.5. Wings.....	18
3.6. Electronics and Components.....	19
3.7. Connectors.....	20

4. Razor 1	21
4.1. Launching Method	21
4.2. Dutch Roll	23
5. Razor 2	23
5.1. Center Body Updates	23
5.2. Razor 2 Flight Testing.....	23
6. Razor 3	24
6.1. Stress Analysis	24
6.2. Thermal Deformation.....	24
6.3. Razor 3 Flight Testing.....	25
7. Conclusion	25
Appendix A: References	26
Appendix B: Stability Coefficients	28
Appendix C: Wingtip Data from RealFlight 6.5	31

Table of Figures

Figure 1: X Connector	8
Figure 2: Water Drop Shaped Hole.....	9
Figure 3: Printing Errors Along Aft Spar.....	11
Figure 4: RealFlight 6.5	13
Figure 5: Airfoil Performance.....	14
Figure 6: Launch Hook Locations	18
Figure 7: Razor 1 Wing Structure	18
Figure 8: Razor 2-3 Wing Structure.....	19
Figure 9: Winglet Attachment	21
Figure 10: Car Launch	22
Figure 11: Jet-a-pult Launching System	22

1. Introduction

1.1. Project Background

From crop-dusting to search-and-rescue (Valavanis & Vachtsevanos, 2014), the use of Unmanned Aerial Vehicles (UAVs) has become more widespread as they grow smarter through increased autonomous systems (Saranya, Pavithira, Premasai, & Govindarajan, 2015). The use of UAVs are also becoming more widespread by soldiers in the field (Wagner, 2015), providing real-time surveillance which can be vital in combat situations. These UAVs must be easy to operate, have long flight times, high damage tolerance, and be quickly and easily repaired or replaced. Current aircraft used in this role tend to be damaged easily and introduce supply line problems for replacement parts. The introduction of 3D printing holds the possibility to reduce these supplying problems (Garrett, 2014). Therefore, the Army is looking into deploying 3D printing stations into the field which would be able to produce equipment very close and have access to “libraries” of parts and equipment stored such that the operator can search based on mission the proven designs approved (Breedon, 2013).

3D printing has already created successful flying designs, including one produced at the University of Virginia’s Rapid Prototyping Lab (Easter, 2013). This aircraft, based entirely on converting a Sig Kadet (SIG, 2015) to a 3D printed frame, employed metal landing gear and additional fasteners as well as extensive post-production processing times to add a thin plastic skin to the plastic frame. An entirely 3D printed design by the University of Sheffield emerged approximately half a year after the first successful flight of the Razor, which had a similar configuration and production times. However, that aircraft was an unpowered glider (ARMC, 2014). Later design iterations for this aircraft sported a pair of electric ducted fans for propulsion, but still appear to be catapult launched and is listed as a heavier frame at 7.7lbf (Coxworth, 2014). Another aircraft, called the Hyperion, produced in collaboration of the University of Colorado, the University of Sidney, and the University of Stuttgart, used 3D printing to create molds for a carbon fiber frame rather than to create the airframe itself (Koster & Soin, 2015).

1.2. Problem Statement

Design objectives for the Razor were based on the existing AeroVironment's RQ-11 Raven. Made with an all-carbon fiber airframe, the Raven has a flight time of up to 90 minutes, with a 55 inch wingspan, and an empty weight of 4.2 pounds with a payload of 1.5 lbs of surveillance equipment. Individually, the Raven consists of a \$35,000 price tag for just the airframe with the entire autopilot and ground station systems bringing the total cost to \$250,000 (Army-Technology, 2015). Repair is another area of concern when deploying the UAV. Despite the toughness of carbon fiber, it is difficult to repair, thus damage to the airframe can result in delays for replacement parts and propellers.

Intending to match the performance of the Raven while addressing the drawbacks of cost and accessibility to replacement parts, a modular plane capable of carrying 1.5 lbs of payload for extended flight times was the goal of this project. The final design had to be able to be fully assembled from the printer in less than 30 minutes and avoid the use of monokote. The use of extra materials such as 3D printing support material or externally supplied fasteners such as Velcro or screws had to be minimized or entirely removed, and the aircraft also had to be compatible with an open-source Android autopilot instead of an expensive proprietary one. Placement of components should be simplified and more compact with no additional fasteners.

These design requirements are all focused on maintaining a rapidly printed and assembled aircraft that reduces the skills required to assemble the aircraft to a bare minimum.

Multiple iterations would be made to the sizing of the wings, payload location, and propulsion system placement, based on the capabilities of the printer and the flight characteristics found in simulation software. Solidworks CAD software (Dassault Systemes, 2015) was used to create the internal geometry and generate the files required for the 3D printers.

2. 3D Printing

2.1. Constraints

As 3D printing was the center of the design, almost every design decision was made with this process in consideration. While the possibilities of 3D printing in the near future are vast, this project was limited to equipment and materials available at the University of Virginia's Rapid Prototyping Lab. Therefore, only certain types of plastic and printers were considered for this project. This also meant limited access to experiments with different temperatures and head speeds.

2.1.1. Fortus 400MC Large

Of the printers available, the Fortus 400MC Large was chosen for use in manufacturing the aircraft. It has a printing area of 16''x14''x16''. At the beginning of the project, this was the largest printing area of any of the printers available, with the option of two different types of materials. Over the course of the project, several problems occurred within the printer that negatively affected the quality of the print. These included a fan that stopped working, material clogs on the printing tip, and poor material quality. However, these problems were fixed by regular maintenance to the machine and replacing the material.

Stratasys recommends walls no thinner than 0.04'' on this printer in the x-y plane (Stratasys, 2010). The z-direction of the printer has a resolution of 0.01''. Using the T16 tip on the printer, it was experimentally determined that a 0.02'' wall could be achieved in certain situations. The use of a different size of tip could offer minimum thicknesses of 0.007'' in the z direction and .014'' in the x-y direction, allowing smaller features and sturdier walls at the cost of significantly increased print time. Due to this downside, the smaller sized tip was not used.

Although 0.02'' walls would be printed correctly occasionally, this was not consistent. To solve this, care needed to be taken when generating the toolpaths for each part by doing "layer scans" inside of the software. This meant quickly looking through each layer to ensure that a toolpath was assigned correctly to each wall of the plane. Originally, when toolpaths failed to be created correctly, it was assumed that problems with the method of sizing the skin of the aircraft inside of the software were to blame. In order to assure that the thickness of each wall was at least 0.02'', the walls inside of Solidworks were resized to 0.022''. This solved the problems with toolpaths not being created; however, the software would then place two toolpaths so closely together in order to fit the 0.022'' sized wall that problems in printing would occur. While the parts would print, there were numerous repeatable errors that proved to weaken the structure significantly.

It was determined that the software allowed 0.02'' thick walls only when the toolpath could make a closed loop. For example, a square with a hole in the center can be printed, even if the thickness between the outer wall of the square and the start of the hole was as small as 0.02'', but only if the head could trace continuously and completely the outer contour and end back

where it started. As long as this criterion was satisfied, it was found that the part would print completely and correctly, creating parts that showed no degradation in quality.

Therefore, areas with holes through the skin, such as the hatch and antenna holes cannot be printed thinner than 0.04". The center body was designed such that areas that could not be printed with a fully closed loop would have this increased sizing. Since the spars are two full paths thick from top to bottom of the airfoil, the wings and aft center body sections are completely enclosed and are continued to be printed at a 0.02" thickness.

Another potential source of significant printing errors was the printer itself falling out of calibration. The machine was routinely recalibrated every several weeks, which kept errors to a minimum. This is a simple process that only takes a couple of 6-minute printing cycles to correct, and is expected to become less problematic as 3D printing technology evolves.

2.1.2. Materials

As of the beginning of this project, the Fortus 400MC offered printing in two types of plastic materials, ABS and Ultem 9085. As the support material for Ultem is not dissolvable in a chemical bath, it has to be manually removed, which originally removed it from consideration. However, it was chosen for the entire aircraft once it was found that it was possible to print with no internal support material via the use of careful design.

According to datasheets compiled by Stratasys, Ultem has an ultimate tensile strength of 71.6 MPa (Stratasys, 2013) which was the value used for comparison during stress analysis. However, other sources claim ultimate tensile strengths from 78.6 MPA (Onwubolu, 2014) all the way to 84 MPa (Bagsik, 2010). This could be due to differing printing conditions as well as specific geometries.

The strength characteristics of any FDM-produced component are lessened across the z-direction of printing (Bagsik, 2010). It has been difficult to estimate the actual reduction in strength due to the nature of the thin walls used on the Razor, but during stress analysis performed in Solidworks, a safety factor of 10 was used to compensate for this unknown. Due to very small span-wise (z-direction) forces, and thoughtful integration of thickenings at the joints and tapers to normal wing size, this rather generous estimation failed to pose a significant design challenge.

2.1.3. Part Orientation Due to Grains and Airfoil

With the intention to maintain the integrity of the airfoil shape by tracing it out with a single grain, it was decided to print the external components of the airframe with left and right sides up/down. This presents a less rough surface to the oncoming flow than any other orientation, as well as increasing toughness due to fewer grain edges. However, it presents some weakness on the center leading edge across the z-direction upon landing. With the hatch that splits up the length of the grain along the front, a hard landing on the ground can cause layers to split.

The engine mounts required a different printing orientation. As designs for mounting have always included complete enclosure around the motor, printing them in a tail-up/nose-down orientation was chosen. As well as allowing for thin loops around the motor, this orientation also gives a strong spring-loaded nature which also helps in securing the motor.

The primary connectors' printing orientation has been a source of some discussion over the course of the project. These components, shown in Figure 1, extruded dovetailed connectors in the shape of an extruded X, are used to hold the three major sections together by sliding the

top/bottom half of the X into a holder on the wings, then sliding the center body onto the other end. The original orientation had a top-down view from inside of the printer down would show the X, but this was found to be too strong. While this component was a designed-to-fail point between the wing and center body, this orientation completely removes the z-direction weakness which results in either the wing/body breaking or the x connector being ripped out of the socket. Printing the x connector on its side would intrude the z-direction weakness back into the design. However, it could introduce too much weakness, and was thought to be able to snap under normal flight loadings. Therefore, the original orientation has been continued.

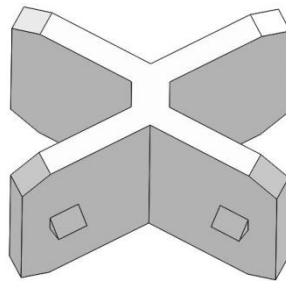


Figure 1: X Connector

2.2. S3D

2.2.1. Support Material

When printing, each part starts from the base at the tray and is built upward. If a higher layer has nothing from a lower layer of the part on which to build, such as a very steep overhang or a separate structure that connects on a higher layer, then support material is required to hold the model material as it gets printed. The standard angle for overhang that requires support material is 45 degrees as specified in most tool pathing software. This can be manually changed inside the software, but doing so can quickly lead to malformed components when printing.

After printing, support material is removed by either manual removal or by the use of chemical baths which dissolves the material away. However, at the time dissolvable support material was only available for ABS plastic, and not for the Ultem 9085. Support material is generally priced the same as the model material which means additional costs can quickly add up for what could be very little difference in components based on one needing significantly more support material. It also increases printing times significantly as well as introducing the times of post-processing such as the chemical baths or prizing the material off with pliers.

Focusing on reducing and removing support material, early experimentation with printing overhang angles and modified geometry promised results that exceeded expectations. The first wing piece printed tested the reliability of the tool-pathing software and printer to produce very tall, thin self-supporting structures that do not require support material. After this successful proof-of-concept print, an additional requirement was added to the project to use support material at only specific designed-to-break sections. This drastic support material reduction accomplished entirely through strategic placement of model material on lower layers was termed Self-Supporting Structure Design (S3D).

2.2.2. Part Orientation due to S3D

Overhangs of angles greater than a setting within the toolpathing software, generally defaulted to 45 degrees, automatically add support material. This automatically rules out printing complete circles in the x-z or y-z planes (vertical orientation). However, as long as triangular

notches are added to the top of the circle at an angle where this limit is not exceeded, a similar shape can be printed. This distinctive “water drop” shape as shown in Figure 2 allows holes through the plane to be printed. This is utilized for the pitot tube and antennas.

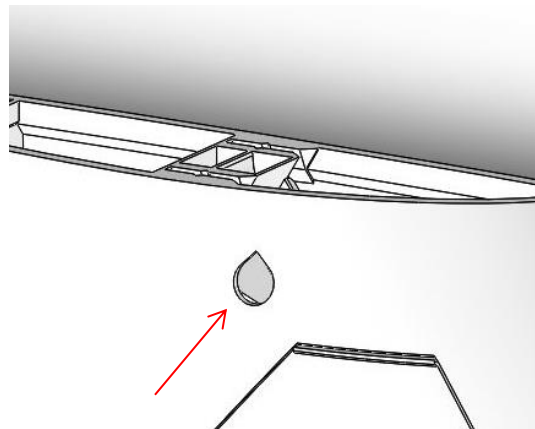


Figure 2: Water Drop Shaped Hole

S3D changes internal structure, by requiring “growth” of each internal structure from a nearby wall. It was found that upward-facing x connector holders could easily be grown from the walls as well as the main spars around them. The only downward facing x connector holders that could be printed needed to be directly touching the build tray. This means that features that stay very close to the outer wall of the aircraft inherently have a lower associated cost in terms of weight, printing time, and vertical space required than features at the mid-thickness line. Thus, attachment points are pushed outward to the walls of the airfoil cross section, and features that have to cross the centerline are generally extended as far as possible in the vertical direction to get the most benefit for the higher cost.

2.2.3. Break Away Sections

In order to print the top hatch in place simultaneously with the center body, the top and bottom sides of the hatch required a wall that could be reliably and easily sheared off along a line. The original idea of printing triangular holes very close together to allow a flat, horizontal section to tear off proved to be difficult to remove and led to consistent printing errors in those regions. This also left the two components as one part inside of the CAD software, leaving some difficulty in separating the two for visual and replacement part printing reasons.

A different method is to allow a very limited number of layers of support material to be printed between the body and hatch. This proved to allow significantly more accurate printing and simpler removal. It was found that the lower feature of such a breakaway region needed to be printed at least 0.02” wider on all sides than the upper wall. Such sizing left a 0.04” thick skin growing in size to 0.08” table, on which a 0.04” spacing of support material held a 0.04” thick skin. This was found to leave such an easily removable section and is so well supported during printing, that this method was used again for a phone camera hole in the bottom of the plane.

2.3. Printing Problems

2.3.1. Warping of Parts

The single largest problem encountered during the printing of the Razor has been the warping of components, both during printing and as the components are taken out of the machine. It has affected how components are placed on the tray to be printed and how many at a time can be printed. While there are concerns about the impact that warped components can have on the aerodynamics of the aircraft, in practice, it does not seem to have any major effects, and is thought to only be noticeable over very long flights.

As any part is printed, the printer must maintain a very warm environment inside of the printing area to keep consistent conditions. Otherwise, the base of the part may cool and shrink, resulting in printing errors. To this end, the printer keeps constant airflow of heated air across the printing area. However, if the printing area is then filled with very tall, thin aerodynamic structures, the airflow will be affected. It has been observed that when wings and elevons are printed very close together; they usually have significant warping by the end of the print. This is what has kept an entire Razor from being printed in a single run of the machine.

This airflow has also completely destroyed a test print. When trying to print a square structure in the x-y plane to the thickness of 0.04'', a tall, thin wall with several small holes was presented to the oncoming flow. The areas around these small holes ended up with a very poor print quality, as the material was bulged out and not printed correctly on a straight line. Therefore, wide, thin walls perpendicular to the vector of the oncoming flow are now avoided.

Certain geometries were found to significantly increase warping. Very thick structures on top of, or joined to, thin walls result in the thinner walls cooling faster than the thicker regions as the part is removed from the printer. The smaller amount of material in the thinner sections also allows more warping to happen, thus leaving these sections extremely vulnerable. Early iterations of the Razor incorporated longitudinal stiffeners in the body section for stiffness which subdivided the surface of the body into square sections of about 4'' by 4''. These subdivided sections tended to always be badly warped, but removal of those sections has since smoothed those areas back out.

Even consistently thin sections such as the elevons will often end up badly wrinkled along the z-direction of printing. As there was no structure to remove on the elevons, other ways of reducing the warping had to be considered. Rotating the elevons 180 degrees such that their trailing edges are pointed into the oncoming flow inside of the printer has consistently shown to have only very small amounts of warping. This has led to the standard orientation of the T.E. of the aircraft being pointed into the oncoming flow as well, with similar results.

As the printing head is placing down material, it does create a force on the part being printed. When the layer is very large with a thick base this force is negligible. However, with very small (0.08''x0.08'') features, these forces are significant and it is common to see them deflect temporarily as well as vibrate during printing. Occasionally, this deflection can lead to plastic deformation. Once this happens, the printer will not be printing directly over top of the previous layer, leading to misaligned features which can snap easily. One example was an elevon (all walls thinner than 0.04'') that experienced such a shift, placing an upper layer almost an entire wall thickness (~0.01'') offset from the lower layer, resulting in only a very weak bond holding the two layers together. This elevon came apart easily out of the printer and was clearly not flight worthy. To prevent this, printing structure much stronger and less likely to flex on smaller parts is important.

2.3.2. Removing Components from Tray and Attachment Sizes

At the beginning of the project, there were problems with the removal of very short, flat parts from the build tray. This was mostly a problem for the winglets, but was also a concern for several small connecting pieces used on earlier versions of the Razor. These problems were solved mostly by removing all of the flat connectors, and by chamfering the down facing edges of the winglets. This gave a strong corner from which to lever the part off of the build tray.

Another problem that can arise from the printing head is that with narrow (0.1”) but rather long (>3”) bases, the component can be ripped either partially or entirely off of its base. When printing hatches separately, care had to be taken to keep this from happening, as often the corners would pull upward off of the bases. Wider bases, more curvature, and support towers printed along the side of the hatch that were removable after printing helped keep them printing correctly.

2.3.3. Unexplained Printing Errors

Other printing errors that cannot be adequately explained by any of the previous problems have also been encountered. When printing an aft portion of the center body, the toolpath travels along the outside of the aircraft, then turns and runs down along the internal spar. There was a stretch of printing in which these areas right at the bend would end up separating, leaving a line of holes just above and in front of the spar as shown in

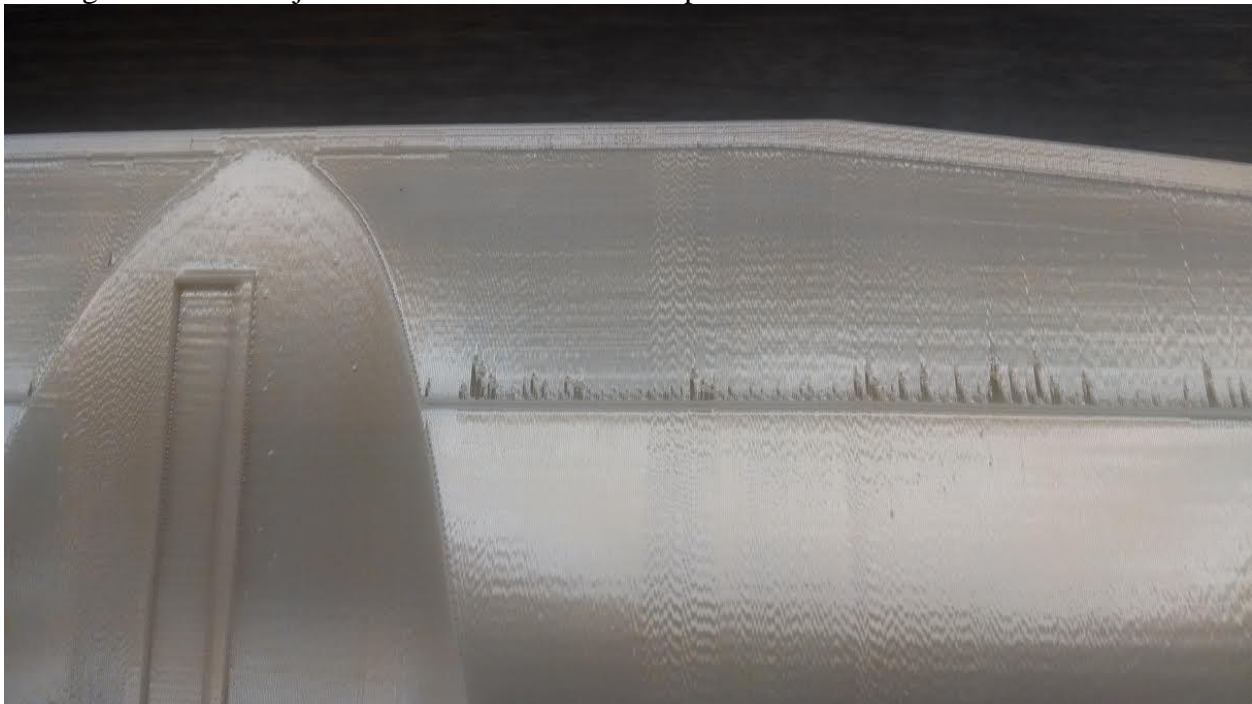


Figure 3. There did not appear to be any other problems with the printing head or material, and eventually, these errors disappeared. The only factor that had been changed was that greater care was taken in the placement of parts during printing, as parts printed in the far back and forward middle have done better on average.

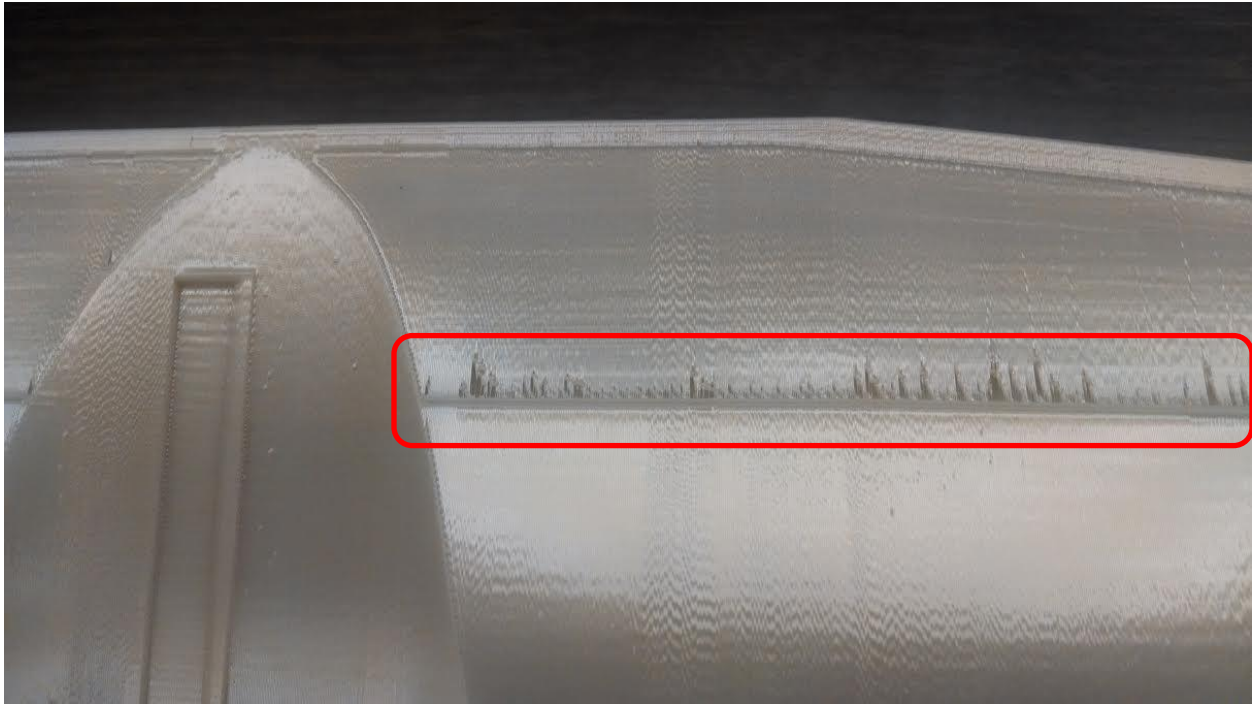


Figure 3: Printing Errors Along Aft Spar

3. Technical Aspects of the Design

3.1. Aerodynamics/Sizing

In order to match the capabilities of the RQ-11, the aircraft needed to be backpackable, simple to assemble, damage tolerant, and lightweight. Therefore, trade studies were performed between three different planforms: conventional, canard, and flying wing configurations. The conventional configuration allowed for simple aerodynamics and analysis, but was quickly ruled out since it required printing more components such as multiple fuselage and tail sections, which would have meant more weight and parasitic drag. A canard configuration offered only a marginal improvement to the overall aerodynamics of the aircraft by making the stabilizing force from the “tail” a lifting force rather than a downward force. However, it also has the same downsides as the conventional configuration, as well as being a less commonly used planform and thought to have poorer stability characteristics.

The flying wing configuration, by contrast, offered less overall drag by having less external flight surfaces. Without separate tails or fuselage components, there is a minimum of surface area to create friction with the air traveling over it. A flying wing also integrates all of its structure with the wing, meaning thicker structure locally, but less overall, dovetailing with FDM printing capability of having denser material with minimum printing sizes. It also means fewer components, as it was found that the Razor could consist of building up only three major sections. This includes a center body section that would contain most of the electronics, and two wings with winglets. With only two major joints, the Razor would reduce inherent joint weakness, and be a more structurally robust design.

Once the planform was chosen, preliminary sizing was based on estimates for the weight of the airframe as well as for the batteries and payload. It was decided to keep the wingspan shorter than five feet to keep hand launch simpler and the portability high. The initial design had a 42” wingspan which kept the aircraft contained to three major sections, each of which was

later sized to a span of 16'', the vertical printing area of the Fortus printer. Therefore, the overall wingspan was raised to 48''. The angle of sweep and washout on the wings was then set to make the airplane stable, using a combination of equation-based estimates and flight simulations in RealFlight 6.5 (Great Planes® Model Mfg, 2013).

For reasons of simplicity during the initial designing phase, a constant airfoil was used over the entire wingspan. After reviewing several airfoils, the E344 was chosen due to its favorable flying wing characteristics (Eppler, 1990). It also had the greatest thickness of such airfoils, allowing more internal room to store electronics, removing the need for additional nacelles or other disruptions to the airfoil shape.

Finding the correct location of the center of gravity (CG) was expected from the beginning to be the most difficult part of a flying wing configuration. Therefore, most of the early work was centered on finding ways of computing and simulating the longitudinal stability. Code was written to take the planform geometry and airfoil data, and discretize the wing into many sections along the span. Lift, drag, and moment from the airfoil was computed from each section and summed together. A movable point representing the CG summed the moments from the lift offset by the sweep and the moments from the airfoil then generated a static stability curve shown in Appendix B. The movable point could then be slid until this plot showed a sum moment of zero at the correct angle of attack.

3.1.1. Initial Simulation

A rough model of the initial estimated geometry of the Razor was created inside of RealFlight 6.5, shown in

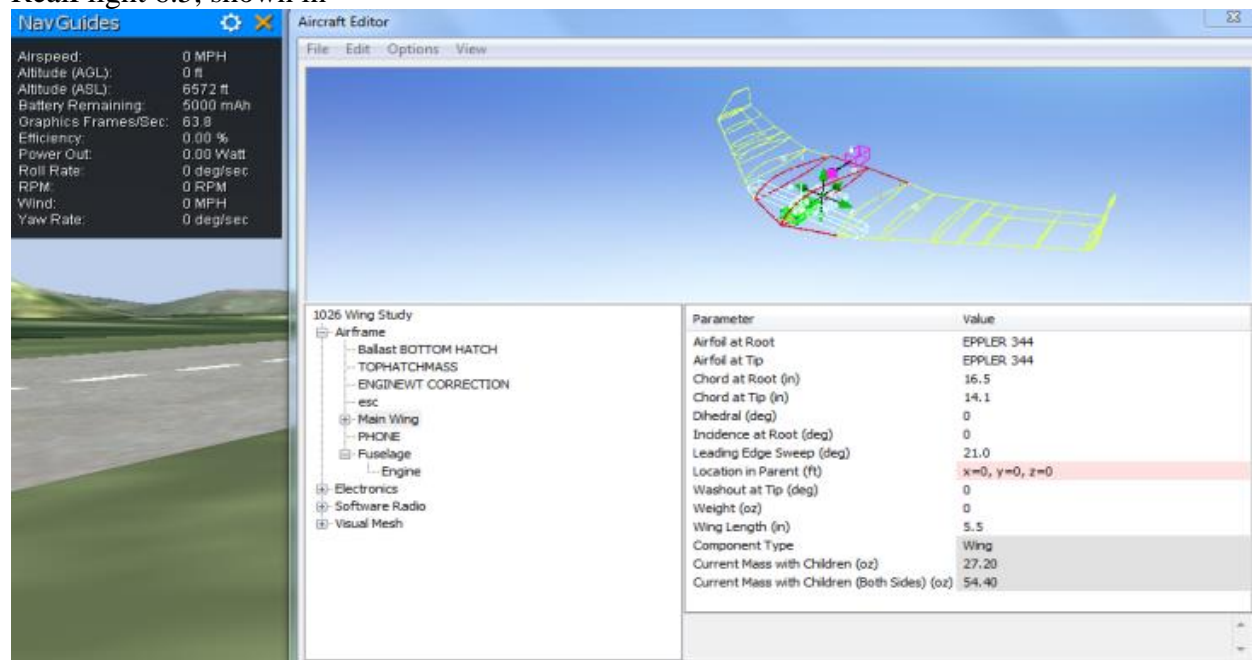


Figure 4, to test more quickly and cheaply the stability of the calculated aerodynamics. Those involved with this project had previous experience with the software, and was confident of its accuracy for the relevant flight regimes. This model incorporated the preliminary airfoil selection, a ducted fan motor tuned within the software to give the expected amount of thrust, and large control surfaces for the early tests. After a few initial tests and iterations within the simulator, it showed that 4 degrees of washout at the wingtips were necessary to make the plane

longitudinally stable at the correct angle of attack. In addition, 42 degrees of sweep was also necessary to move the center of pressure back to keep the plane stable.

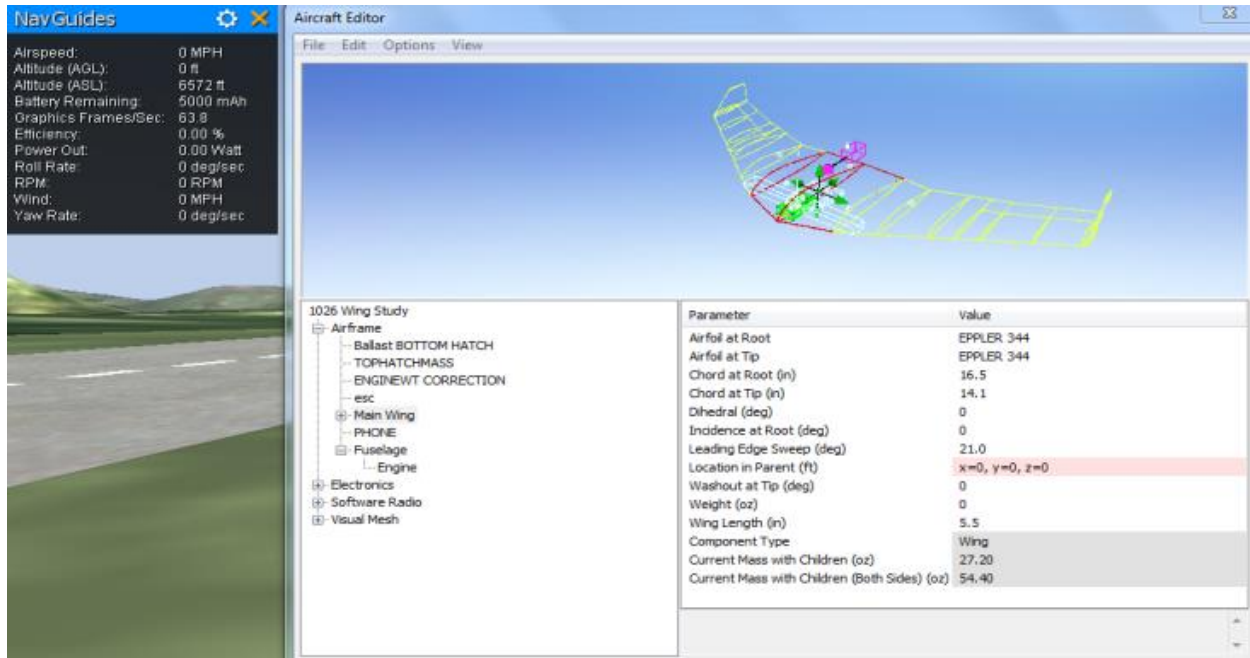


Figure 4: RealFlight 6.5

In these simulations of a hand launch (which started the aircraft at 25 mph at about 4 feet in the air), if the aircraft failed to rotate nose upward properly for a successful take off, then the current CG location was in front of the forward limit. Alternatively, if the aircraft rotated too far into a stall or it was impossible to push the nose back down to a proper attitude, then it was behind the aft limit. By testing several locations around the Excel predictions, stability ranges were found empirically. Then, the up/down angle of the motor was tested by putting the plane into a steep dive. If the plane recovered itself quickly, the angle was too far down. Conversely, if it continued rolling downward into a steeper dive, the angle was too far up.

3.1.2. RealFlight 6.5 Optimized

Extensive research on airfoils and the amount washout at 2, 4, and 6 degrees of twist at the tips through analysis using maximum flight time as the objective generated data compiled in Appendix C that guided the optimization of the geometry. In order to get quantifiable data from RealFlight, two different methods were used. In the first, the aircraft was first taken to 35 mph flight in steady level flight (SLF) conditions. Then, the flap setting was set to neutral, and the throttle was adjusted until the aircraft again entered SLF. In the second, the aircraft was put into SLF at a number of airspeeds, using a combination of throttle and flap settings, in order to get a full spectrum of aircraft performance.

As RealFlight gives in-flight telemetry such as airspeed, altitude, power output, and battery remaining, SLF was known when airspeed and altitude were constant and neutral flaps were a known knob setting on the controller. As no autopilot option within RealFlight is known of, this all had to be done manually with occasional corrections in the roll direction. Therefore, each data point was fairly expensive to get in terms of time. For example, obtaining data from the first method could take up to a half an hour for a single given configuration and its washout variants. The second method could take well over an hour.

In order to keep time spent on the simulator productive, the first method was employed on certain archetypical airfoils to identify trends. The second method could then identify amongst the most promising candidates which had the most favorable flight characteristics. While the specific numbers (such as the calculated flight time) were not expected to be realistically accurate when compared against real life, the internal consistency was expected to hold. Thus, a thicker symmetric, a thin symmetric, a positively cambered, a negatively cambered, and a very thick airfoil with a slight amount of reflex were chosen for study.

When the thinner, negatively cambered airfoils were shown by this early testing to have the highest flight times, ranges, and CL/CD , where the highest performance is represented by the upper right hand corner of Figure 5, more emphasis was put into airfoils with those characteristics. As there was a very few number of those in the RealFlight library, this helped reduce the amount of testing even further. When the selection came down to MH 49 and the MH 110, they were given the full analysis of the second method. Ultimately, the MH 49 was shown to be consistently superior across all flight speeds to the MH 110, and the former was chosen.

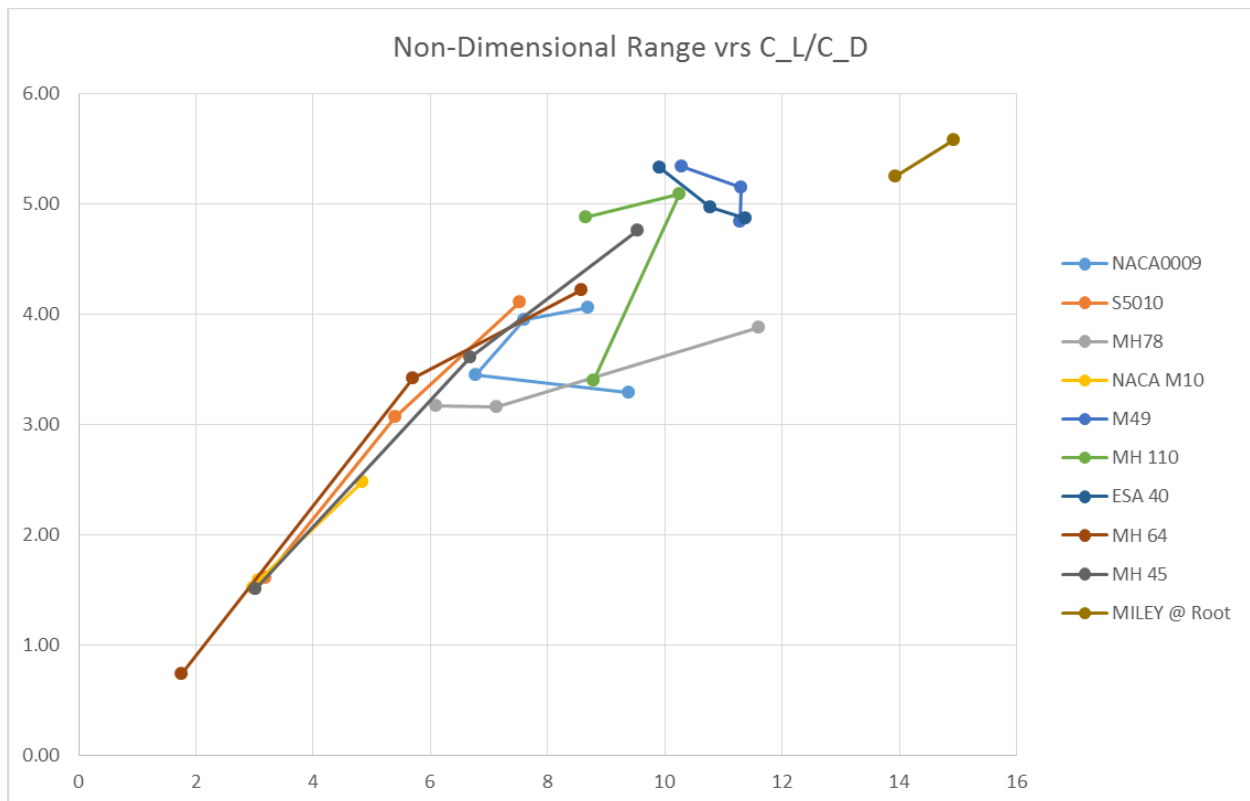


Figure 5: Airfoil Performance

Based on a recommendation by flight testers at the Air Force Academy in Colorado and once found in the RealFlight airfoil library, the Miley M06-13-128 was tested as a replacement for the root airfoil. While in a direct comparison to the original E344 airfoil, it showed improvement in CL/CD and power requirements, the actual geometry of the airfoil was slightly thinner at the point of max thickness and narrowed faster aft of that point. This showed that a change would make internal placement of electronics and payload much more difficult. Thus, the Razor continued using the E344 in combination with the MH-49.

It was assumed that RealFlight linearly transitions the airfoil characteristics over the section geometry, such as the lift and drag created by that section. As this may not represent the real life effect of transition, the effect of making this section as small as possible and placing it either further out or closer in on the span was studied. In the interest of keeping the amount of study on this reasonable, due to the large amount of variability (length, location of transition) that could exist, it was decided to only analyze the effect of transitioning over the entire MH 49 section, the inner half, and the inner quarter. While the data showed a transition over half of the wing was optimal, it was decided to transition the airfoil over two inches as inboard as possible to keep the control surfaces from having an overly distorted shape.

While there was study on the control surface sizing inside of the simulator, they were ultimately sized as small as possible while keeping the servo entirely buried in the profile of the wing. As the axes of the control surface and servo horn are collinear, making the % of cord or moving the inner bound outward would result in the servo getting pinched out by the local airfoil. However, this still results in fairly largely sized elevons, which have been proven to give the control necessary for the aircraft.

During simulations the airplane would roll slightly off of level and need to be gently corrected. This seemed to imply that the Razor was very slightly unstable in that direction. When discussing if this tendency was actually a problem, it was decided to see if adding dihedral would make it stable. However, when even 5 degrees of dihedral were added first to just the wings, then later over the entire aircraft, it still failed to remove this effect. Both moving the vertical location of the CG and using even more extreme numbers of dihedral also resulted in either no effect and making the aircraft unstable in the longitudinal direction. While it was never determined if RealFlight simply struggled in computing roll stability or if there were no ways of practically making it stable, it was determined that the problem was insignificant enough that either the pilot or autopilot could quickly correct. Therefore, the aircraft was left at zero dihedral.

3.2. Weight and Balance

3.2.1. Components and Placement

The heaviest electronic components in the plane are the batteries, motor, phone, and electronic speed controller (ESC). As the batteries are by far the heaviest, nearly half of the empty weight of the Razor, and had to be placed as far forward as possible to offset the all of the weight of the wings aft of the CG. This meshed nicely with the E344 airfoil reaching max thickness fairly far forward, but there were still problems with the batteries being held further back than desired by being “pinched out” by the leading edge.

The motor had to go towards the back of the airframe, due to the vertical distance of the thrust line from the centerline of the airfoil becoming too great. This would create problems of too much overturning moment, which affected stability. It was decided that aft weight penalty was worth not having to cut an airflow channel directly through the thickest section of the airfoil, and decided to keep all of that space for internal components.

The phone has always been located as far forward as possible. Once it was decided to have two batteries, they were split apart and the phone placed long ways along the chord line between them. On earlier version of the tray, the phone was placed toward the very bottom of the aircraft. This was to give the phone the best place for the camera to look out of a hole on the underside. Later on, the phone was moved to the top of the tray for ease of accessibility upon opening the hatch.

Outside of these, the ESC is the heaviest electronic component and as such, was originally placed in front of the phone, due to its smaller size. However, the high current wires create strong EM fields, making it crucial for the autopilot electronics that it be placed as far aft as possible to keep these high current wires short to limit these fields.

3.2.2. Tray Design

In order to keep the rest of the lighter electronic components held together and locked down to the airframe, a tray that would lock in at the center of the aircraft was designed. Accomplished first by sliding along X-connector rails placed on either side of the bottom hatch, the later versions of the Razor revisited this broad design multiple times. However, specific sizing on the tray had to be redesigned with every change in either the airframe or electronic components, which was one of 3D printing's advantages, as the tray could rapidly change to keep up with the changing electronic requirements.

In the latest version of the Razor, the tray was designed with special care around snapping components directly in. Wiring around such a frame has been difficult, but the tray has been designed to make this process simplified, while ultimately surrounding and trapping the extra wire to keep the interior of the aircraft uncluttered. When the phone was moved to the top of the tray, a special channel was designed into the tray to keep anything from sliding in the way of the camera, giving it a clear picture out of the bottom of the aircraft. This channel was also designed to allow cooling airflow through the center of the aircraft.

3.2.3. Payload Placement

While internal mounting pylons for payload have never actually been added to the design, there are clear areas just behind the batteries on either side designated for payload. An effort to keep the regions directly over top of the CG open have resulted in two 2.5''x3.75'' bays split by the motor scoop. Therefore, up to 1.5 lbf can be placed into a Razor across those sections with small effects on the aircraft's aerodynamics and stability. However, this payload has to be fairly compact and robust in order to fit within the airfoil's thickness.

3.3. Propulsion

When choosing a propulsive system for the Razor, it was decided to use a ducted fan system in order to protect the moving plastic parts and hands during launch. Propeller aircraft are notorious for needing replacements often, as long exposed blades absorb damage quickly and easily. It can also create supply line problems for troops in the field; completely grounding surveillance aircraft regardless of overall condition if there are no available working propellers. Conversely, ducted fans seat the blades inside of a rigid case, and usually never need replacement.

Preliminary sizing for the ducted fan, based on research on currently available models, showed that a ducted fan of approximately 64 mm to 70 mm could be expected to require a 4 cell battery and provide about 2.5 lbs of thrust. After purchasing the model in this range that was advertised with having the best thrust to weight ratio, testing with a scale and a simple test rig showed that it ultimately only gave about 1.2 lbs of static thrust. However, this motor was still flown in Razor 1, and was still able to break 100mph in a short dive.

For Razor 2, a more powerful motor was required. An all metal ducted fan was found with a plastic rotor that weighed considerably more than the previous motor that was primarily plastic, but gave 3.2 lbs of static thrust. This ultimately gave the thrust required for a hand

launch. There were concerns about decreased flight time, due to the higher weight and power required. However, during steady level flight, the throttle could be set lower than with the previous motor which had a much smaller current draw and less battery drain. Wind tunnel testing of the motor running at the expected required thrust output and airspeed yielded promising flight times.

3.4. Structure

The Razor has relatively thick skin compared to other aircraft of its size and only two thin spars as the skin is printed directly onto the frame, completely forgoing any conventional rib structure. This extra, rigid material along the profile of the airfoil gives the Razor excellent strength in both bending and torsion. The thicker skin (0.04") also helps with the damage tolerance of the aircraft.

Until the center body redesigns of later versions, the center section of the Razor was printed in two pieces each starting a wing joint and pressed together at the mid-line of the aircraft. This was done partially to allow for the motor mounting method used at that time and to add another inch in wingspan to the center body to give more internal room for fitting batteries and electronics. Concerns about torsion in the joined sections lead to the addition of longitudinal ribs at half the span of each half center body. Due to S3D, these ribs could not be flat walls and instead were essentially thick plastic bands that traced out the airfoil just under the skin. A cross section of these bands would show a right triangular shape, where the hypotenuse is the skin, and the 90 degree corner is on the inside. Each wall of this band had a thickness of 0.06".

Ultimately, this additional structure was not necessary once the center body was printed as one piece. This band of material also created extensive warping problems for the skin below as the offset of the 0.06" surfaces on top of the 0.02" walls pulled and warped the skin during both the printing and cooling processes. Therefore, as the extra strength was not required, the extra structure was removed.

It was decided that the leading edges of the wings needed to be thicker than the skin of the plane to help maintain the curvature of the leading edge, as well as strengthening the areas of the wing most likely to undergo impact. As the higher curvature regions of the wing are the ones that generate the majority of the lift, the forces of flight are stronger, warranting that the forward 1.4 inches of the chord from the tip of the leading edge be thickened to 0.06 inches. After several unsuccessful landings involving the plane crashing through underbrush, the wings have proven to be very strong and almost always sustain no damage to the leading edges, with the exception to the leading edges in front of the hatches on the center body section.

Although the design requirement was for the Razor to be hand-launchable, the reliability of this method has been questionable on multiple occasions due to the Razor's weight, prompting that launching hooks be installed on the underside of the aircraft. This allows a tensioned spring line catapult system to easily attach to the Razor's frame. This became the primary method of launch for the Razor for a period of time, until hand launch was proven. However, the hook remains on the aircraft in later designs to retain the option of a catapult launch.

The hook is printed approximately 1.5 inches in front of the center of gravity location on the bottom of the center body, shown in Figure 6. It was intentionally placed close to the CG so that the Razor would experience rotation despite the launch cord on take-off. It was sized to a thickness of 0.15" thick and protrudes 0.25" from the skin of the aircraft with the walls chamfered out to 45 degrees for S3D. The hook takes advantage of the additional structure in the region of the CG for testing balance of the aircraft.

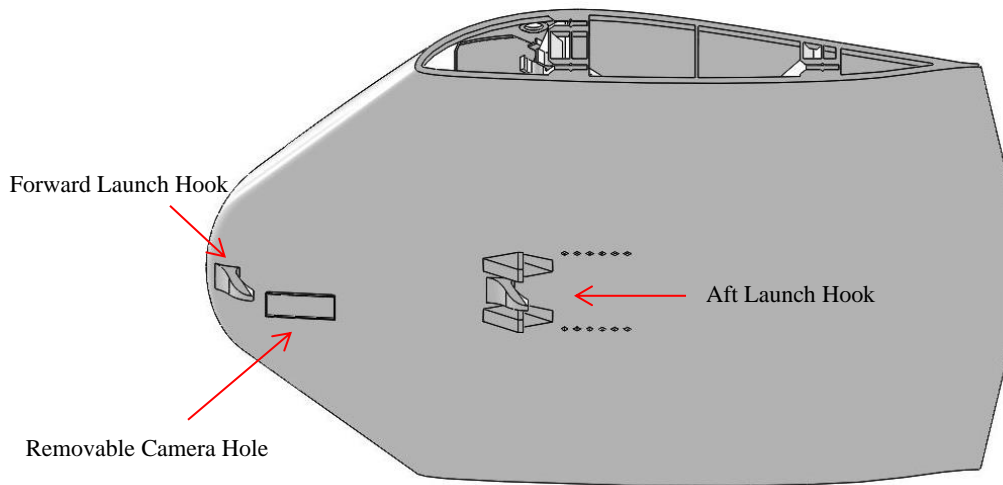


Figure 6: Launch Hook Locations

3.5. Wings

The most structurally intense section of the aircraft is the joint areas between the wings and center body. They were originally printed in a fairly thick manner, as the x connector holding features were tightly connected together. A thick rectangular spar spaced 0.2'' above the bottom of the airfoil ran directly all the way forward and aft as well as multiple rectangular spars more running from top to bottom to keep the airfoil from buckling as shown in Figure 7. This was overbuilt, as minimal loads were shown to be transmitted through the spars, so a much more minimalistic redesign left only a thickened parameter and braced x connector holders, shown in Figure 8. However, this resulted in the weakening of the structure to the point where the wing joint would deform under loading to the point where the x connectors would pop out easily. This created the problem where the wings would pop off during take-off. Therefore, structure has been added back on, thickening the perimeters to 0.2'' as well as adding back in vertical braces in the center of the wing.

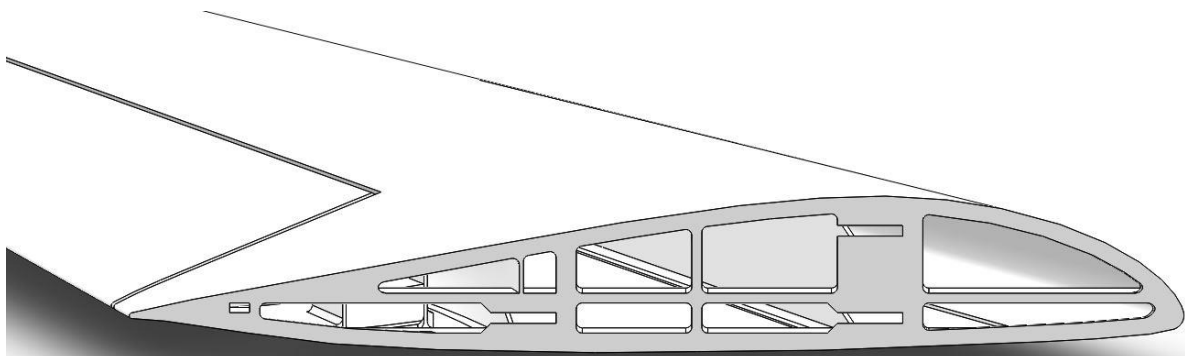


Figure 7: Razor 1 Wing Structure

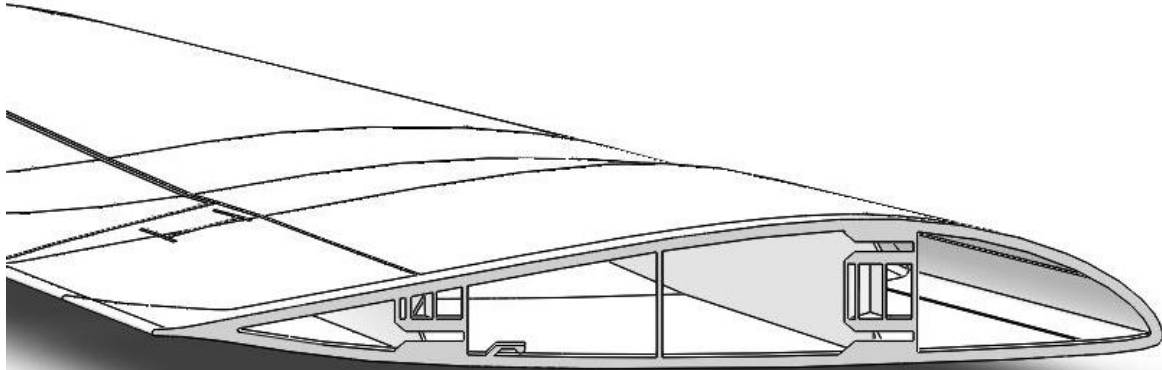


Figure 8: Razor 2 Wing Structure

Due to the modularity of the design, there was discussion early on about where to place the elevon servos, as it would be advantageous to keep all electronics confined to a single section. However, this would require the use of control rods that would be either external on the bottom of the aircraft, on top of the aircraft, or entirely internal. Having a control rod running out of the bottom would introduce damage concerns during landing, while running the rods out of the top was thought to overly disturb the airflow. The internal placement would mean protection during landings, as well as not disturbing airflow, but gave concerns about torque and complexity of construction. Eventually, all three of these options were rejected in favor of servos buried in the wing directly along the axis of the elevon rotation, with direct attachment of the servo horn.

For additional structure on the wings, thickened webbing printed directly onto the skin rather than using conventional spars was considered. However, the test print warped during printing and the toolpathing of the webbing created divots on the outer surface of the wing due to the thin skin. The test wing using the standard support spar was considerably more successful and led to this structure being selected. As there was no need for additional structure beyond the spar, the webbing was removed and the skin was printed as thin as possible. To increase the durability of the skin the leading edge was initially thickened to 0.06 inches to help protect during landing. It was later found that so much additional thickening was not necessary, and scaled back to .04 inches thick.

3.6. Electronics and Components

In order for the plane to be manually flown, it needs to have established contact with a remote control radio on the ground. The DX7s® was chosen and a matching receiver was placed on the aircraft. A pair of Spectrum® servos were originally used to control the elevons, but replaced once multiple servos proved often unreliable by “stuttering” once connected but under no loading. This made them simply too unreliable and were unacceptable. Therefore, Futaba® servos were substituted and have given no problems during the project.

Between the receiver on the aircraft and the motor is the ESC, into which the two 5400mAh Thunderpower® batteries are plugged. When not flown in R/C only mode, the autopilot system is plugged in between the receiver and other electronics. In the first versions of the Razor, the ArduPilot® was utilized, but as the PixHawk® has come out since then, that has replaced the autopilot system used. For navigation, the PixHawk® uses external plug-in

packages to sense airspeed (pitot tube and air pressure sensor), and GPS. The autopilot system connects to a laptop on the ground via its own telemetry radio.

3.7. Connectors

A secondary design goal for the Razor was to avoid the need to purchase additional connectors, such as screws, Velcro, or glue. Necessarily, various connecting methods were designed to lock each component in place on the aircraft, and to hold the three major sections together.

The x-connector was the first of the connection systems designed for the Razor. Intended to be an all-purpose, lightweight connector that could be a designed-to-fail point between the wings and body, it originally also served as the mounting point for the internal tray as well as a longer version for the engine mount. Early experimental 1'' versions showed that a connector of that length could hold up to approximately 60 lbf in direct tension before breaking. Offsetting the connector from the loading line by 1'' reduced the maximum load by about half. As this was overbuilt for our aircraft, the x-connector was reduced to .65'' for earlier version of the Razor, before being reduced in size again to .5''.

The x-connector's shape was exactly as the name suggests, as it is simply 0.04'' walls at 30 degrees from horizontal that extend .2'' from the centerline. A small bump was added to the center of the contact sides to lock the connector in place. When concerns arose during Razor 2 that the x-connectors would slip out of holders too easily under loading, braces were added inside of the walls to keep them from deflecting inward.

Mounting the motor on x-connectors was only possible when printing the center body in two parts, due to the nature of its required printing orientation. In Razor 2, this section was to a single part, requiring a new connection method. Ultimately, a mount design was chosen that wraps around the motor and is locked tight by sliding it chordwise into a thin rectangular slot on the center body, and held in place by a backstop on the back of the part that locks into place on the slot. Likewise, the tray also needed a new attachment method. A press-clicking channel printed into the body and matching feature on the tray did a sufficient job of both holding the tray in place and making it possible to locate the part during insertion.

The winglet attachment has seen the most change over the course of the Razor project. The first version used an additional component shaped like a wishbone, placed into a slot on the wing and held the winglet onto the wingtip by ridges on the deformed arms deflected by hand to allow the winglet on and off. However, sizing the winglet was difficult and the finger holds stuck out into the flow. The second design had dovetail fins on the winglet which would slide into the wingtip. A press fit pin was then used to keep the winglet from sliding off on the rails. Some experimentation was done on incrementing the diameter of the pin by .01'' to determine the right sizing with the ridges left by 3D printing. This system performed satisfactorily, but the extra pin was deemed unnecessary and was replaced by a snapping feature shown in Figure 9 printed directly onto the winglet that locks flush with the winglet surface.

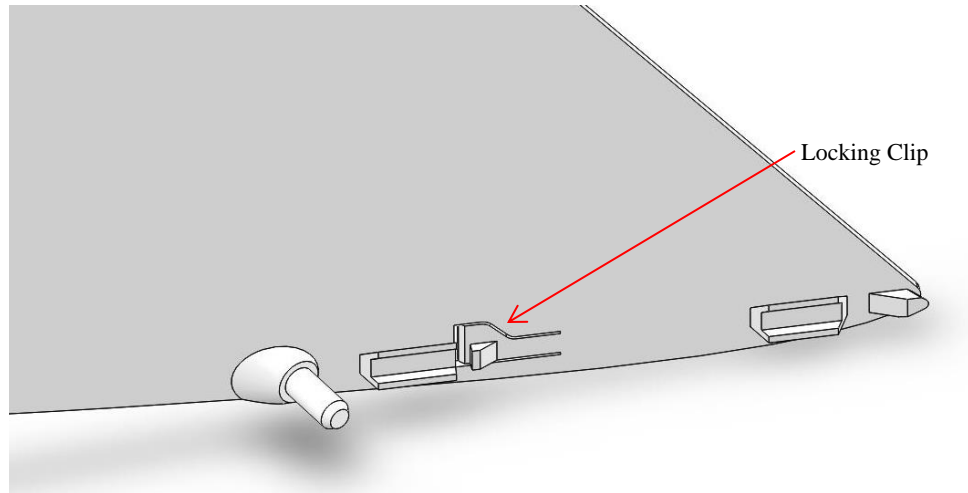


Figure 9: Winglet Attachment

The batteries have always been held in place by the use of a forward and aft wall with either fins or a top wall. This holds them both in place front to back, as well as in rotation. Spanwise motion of the batteries is restricted by the walls of the center body in the outward direction and the tray in the inward direction.

4. Razor 1

4.1. Launching Method

Confidence based off of Real Flight and a preliminary test run that a lightened Razor would successfully take off at airspeeds of at least 20 mph, led to the first flight being launched from a moving vehicle, shown in Figure 10. Holding the Razor through the sun roof, the airplane was released once up to speed and immediately started to climb. It then carried on through the flight, exhibiting stable characteristics. The car launch was then repeated, with the full number of batteries installed, increasing the weight from the previous flight by a full pound. This required the vehicle moving at 25 mph for take-off.



Figure 10: Car Launch

A stationary, repeatable method for launching the Razor was a necessary interim step towards hand launching. The Jet-a-pult, a commercially available launch rail with rubber tubing designed to be staked into the ground and stretched out to achieve the desired loading shown in Figure 11, promised such a launching method. Initial tests with the Jet-a-pult were unpowered and stretched to only 4 and 6 yards to establish the gliding characteristics of the Razor off of the launcher. This distance was then expanded to 10 yards to ensure sufficient force for take-off. The first attempted on a powered launch was successful.



Figure 11: Jet-a-pult Launching System

4.2. Dutch Roll

During the early flights of the Razor, the pilot attempted flight at very close to stall speeds. This made the lateral, Dutch roll mode of the aircraft unstable. Under ideal flight conditions, the pilot could have likely powered up and recovered. However, the plane had turned across the short end of the field, and the pilot was unprepared to react to a Dutch roll. This resulted in the Razor crashing into a tree at around 40mph. This crash resulted in the partial destruction of the center body and one of the wings. The other wing on the plane was also damaged, but was deemed fixable.

Back within the Real Flight 6.5, the model was checked specifically for the Dutch roll. After emulating the flying conditions where it was seen in real life, the simulator did exhibit almost identical behavior. The reason it had not been noticed and corrected beforehand was that it only occurred during an extremely slow flight regime, where previous simulator runs had not gone.

Since the Razor has no controllable rudder and no other reasonable locations for a vertical stabilizer, the size of the winglets had to be increased. Replacements sized at both twice and three times as big as previously were printed. However, after flying with the 2x sizing and observing greatly reduced and easily recovered Dutch roll response modes, that sizing was deemed sufficient.

5. Razor 2

5.1. Center Body Updates

The updates from Razor 1.3 to Razor 2 were primarily focused on redesigning the center body section. Since there had been smaller hatches on both the top and the bottom necessary for instillation of the electronics and batteries, the decision was made to extend the top to a much larger size to allow accessibility to all of the electronics while removing the bottom. This larger sizing was also designed to be designed alongside and printed at the same time as the body, which gave an actual conforming shape than the previously approximated curve. This resolved the printing errors involved with printing the stand-alone hatches as well as the trouble with securely mounting the hatch during flight. The new hatch had six mounting extrusions around its perimeter that fit into fish mouth features on the center body for retention, which allowed for locking features that clip tighter.

With the expanding wings that created more drag as well as increasing aircraft weights and an already underperforming motor, a new motor was chosen for Razor 2. This motor required a new mounting method, as the previous double x connector railings could no longer be printed. Instead, a wrap-around plastic component was designed to be pried open to fit around the motor and then locked tight by mounting it securely into the aircraft. After sliding in along an axis, a deflected beam on the part snapped down into place on the center body and held the mount from sliding out. This method also allows for the motor size to change slightly without creating problems with mounting.

5.2. Razor 2 Flight Testing

Most of the flight testing done on the Razor 2 was to check the proper location of the hook. A metal bar with an adjustable bolt allowed for multiple locations to be quickly tested. It was found that a hook on the leading edge left the aircraft unable to properly take off. It was not until the hook was moved to within an inch of the CG that the tow hook allowed the Razor to

properly rotate on takeoff. The hook was then incorporated directly into the design of the center body by printing a solid plastic hook protruding from the center of the body. This region on the body was also thickened to support the pull of the catapult line. Simple tests were then performed on the new structure by launching at full throttle and flying as normal until the point where the aircraft is clearly successfully taking off, then powering down and landing immediately. The two tests, one of which was empty of payload weight and the other at full take-off weight, both revealed the Razor to have great power and control authority during the take-off launch.

The pilot indicated after flights that the design iterations had succeeded in improving the flight and handling qualities of the aircraft. It was noted that the Dutch roll was lightly stable and uncommon. The two elevons were always sufficient to maintain control over the aircraft and gave a more than satisfactory amount of agility and maneuverability, leading to the pilot's remark that he would fly the plane recreationally.

6. Razor 3

6.1. Stress Analysis

As the problems with the wings popping off easily had not been fully solved in Razor 2, a more in-depth analysis of stress and deformation around mounting regions was performed. Using rigid body analysis suites within SolidWorks, both shell and simplified solid body models were created and meshed both semi-coarsely and fairly fine, respectively. The results were analyzed in overall stress distributions and stresses in the z direction.

On the center body, the largest stresses were around the corners of the hatch and the inside walls of the X connector rails. On the wings, the points of greatest stress were usually the corners where the X connector rails were connected to the spars, which was less of a concern on the center body due to the extra structure required by S3D, leading to the rounding out of all the corners on the wings. However, as the corners of the hatch area could not be practically rounded out due to the thin support material type of attachment used, as well as the inability to fill in any of the inside of the X connector rails, the center body remained fairly untouched by the stress analysis. This was also due to the stresses found on the center body ultimately being much smaller than the yield strength.

6.2. Thermal Deformation

Although thought to have been solved previously by spacing the components out on the build tray, thermal deformation of the part both during printing and removal from the machine again became a major problem for the Razor 3. Major sections of the center body just below the motor inlet scoop became warped inward significantly. The elevons again came out with a regular wrinkle along the z direction.

After reorienting the printing direction such that the trailing edges were then pointed toward the incoming convection airflow, the printing quality of the elevons seemed to be significantly improved. However, the center body still had significant warping, even after rotating its trailing edge into the flow. After discovering that the ESC needed to be moved off of the component tray due to the lack of cooling airflow and overheating problems, it was relocated to this area on the center body. The additional structure required to hold the ESC in place to provide cooling air strengthened the region to the point where this wrinkling has become insignificant.

6.3. Razor 3 Flight Testing

Flights with the Razor 3 utilized a second pilot from the team, and were focused on hand launching the aircraft. While it took several attempts to build the confidence and technique of the one throwing the aircraft, the Razor demonstrated durability and stability. Once the aircraft was successfully hand launched, it was found by the pilot to have good flight characteristics, but with a small amount of difficulty in slowing down sufficiently for a gentle landing without a long, grass runway.

A second flight on another day with the pilot from the Air Force Academy in Colorado did not end as successfully. After multiple unsuccessful attempts, the airplane eventually was launched and began circling the field as normal. However, the ESC overheated and turned off due to the overheating problem, resulting in the pilot crash landing the Razor in a heavily brushed field next to the landing strip. Once found, the airframe was found to be largely intact, only having accumulated two cracks in the center body which were easily repaired.

After the plane was recovered, the next flight was successful in one attempt at hand launching. After circling the field several times, the airplane landed gently with no additional damage. The flight was considered perfect, but was kept short to keep from having problems with the ESC. The pilot reported the same flight characteristics and no concerns.

7. Conclusion

Given a forward lab with a printing system similar to what was available to this project and stocks of the electronics, it is shown that 3D printed aircraft and replacement parts that can produce performance similar to commercial surveillance drones on the market today. Removing many problems of supply lines, production will occur likely very close to the operational area, and directly to the amounts of each component required. These forward bases could quickly identify problems and send back feedback to the designers, who can then send back updated designs.

With two 5400 mAh batteries and an airframe that has minimal wetted area, it will have a substantial flight time as long as it can maintain enough cooling around the ESC. It also has been proven to be able to handle the amount of payload that would easily include several cameras. After significant analysis of the aerodynamics, this aircraft is optimized for flight speeds that give the greatest amount of loiter around a target region. The Razor can be hand, vehicle, or catapult launched, and has the durability to last multiple landings. Available high top speeds and low side profiles will increase the survivability and probability of a successful flight. The team is convinced that aircraft with such properties can have a critical role in both the private and public sectors in the future.

Appendix A: References

- ARMC. (2014, March 28). *3D printing trials of unmanned aircraft at the University of Sheffield broaden the possibilities for this emergent technology*. Retrieved from The University of Sheffield: <https://www.sheffield.ac.uk/news/nr/3d-printing-trials-of-unmanned-aircraft-1.364084>
- Army-Technology. (2015, 4 14). *RQ-11 Raven Unmanned Aerial Vehicle*. Retrieved from Army-Technology: <http://www.army-technology.com/projects/rq11-raven/>
- Bagsik, A. S. (2010). FDM Part Quality Manufactured with Ultem* 9085. *14th International Scientific Conference on Polymeric Materials, September (Vol. 15, No. 17.2010)*.
- Breeden, J. (2013, August 21). *Army preps on-the-spot 3D printing process for the battlefield*. Retrieved from GCN: <http://gcn.com/articles/2013/08/21/3d-printing-repairs.aspx>
- Coxworth, B. (2014, October 14). *3D-Printed UAV now sports ducted fan motors*. Retrieved from gizmag: <http://www.gizmag.com/3d-printed-ducted-fan-uav/34250/>
- Dassault Systemes. (2015, 4 14). *Solidworks*. Retrieved from Solidworks: <https://www.solidworks.com/>
- Easter, S. T. (2013). Using advanced manufacturing to produce unmanned aerial vehicles: a feasibility study. *SPIE Defense, Security, and Sensing, 874204-874204*.
- Eppler, R. (-V. (1990). *Airfoil design and data*. Berlin: Springer-Verlag.
- Garrett, B. (2014). 3D Printing: New Economic Paradigms and Strategic Shifts. *Global Policy, 5(1)*, 70-75.
- Great Planes® Model Mfg. (2013, 2 16). *RealFlight® radio control flight simulator*. Retrieved from <http://www.realflight.com/>
- Koster, J., & Soin, G. (2015, March 3). *Hyperion UAV: An International Collaboration-Presentation*. Retrieved from researchgate: http://www.researchgate.net/profile/Jean_Koster/publication/267269369_AIAA_SciTech_2014_Motivation_Green_Aviation-Presentation/links/544944740cf2f63880811162.pdf
- Onwubolu, G. C. (2014). Characterization and Optimization of Mechanical Properties of ABS Parts Manufactured by the Fused Deposition Modelling Process. *International Journal of Manufacturing Engineering, 2014*.
- Saranya, C., Pavithira, L., Premasai, N., & Govindarajan, R. (2015). Recent trends of drones in the field of defense. *Internat ional Journal of Electrical and Appliances*.
- SIG. (2015, 4 14). *KADET SENIOR*. Retrieved from SIG mfg: <http://www.sigmfg.com/IndexText/SIGRC58.html>

Stratasys. (2010, 6 16). *FDM Design Handbook*. Retrieved from stratasys:
<http://www.stratasys.com/~media/Main/Secure/Applications/Marketing%20and%20Design%20Models/Application%20guide%20-%20FDM%20design%20handbook.pdf>

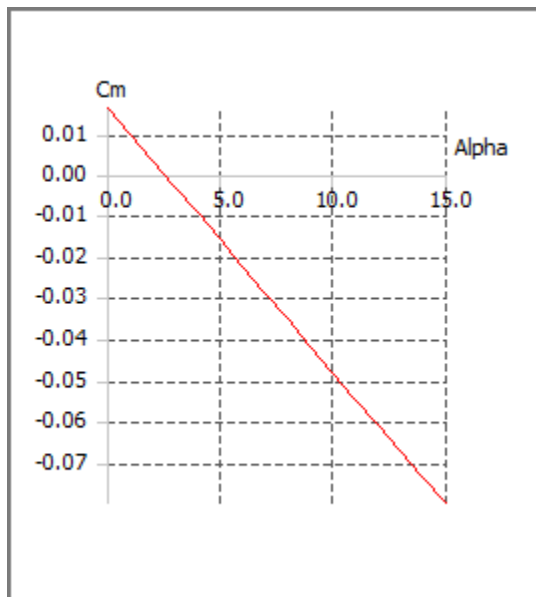
Stratasys. (2013). *Production-Grade Thermoplastic for Fortus 3D Production Systems ULTEM™ 9085*. Retrieved from stratasys.com:
<http://www.stratasys.com/~media/Main/Secure/Material%20Specs%20MS/Fortus-Material-Specs/FortusUltem9085MaterialSpecSheet-US-ENG-1-14%20Web.pdf>

Valavanis, K. P., & Vachtsevanos, G. (2014). *Handbook of Unmanned Aerial Vehicles*. Springer Netherlands.

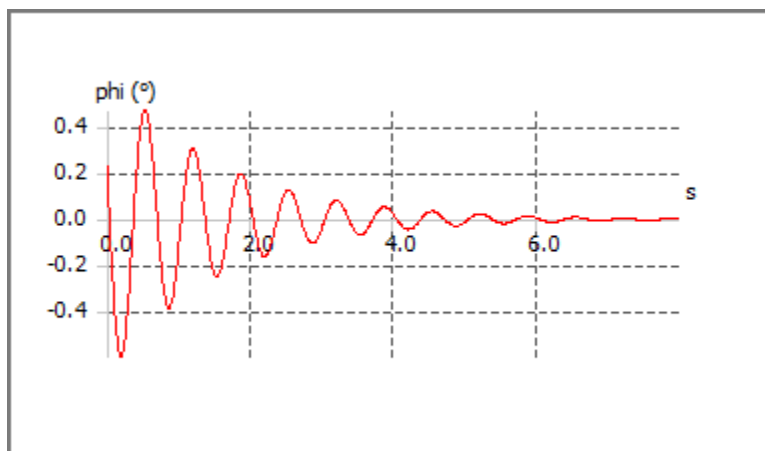
Wagner, M. (2015). Unmanned Aerial Vehicles. *Max Planck Encyclopedia of Public International Law*.

Appendix B: Stability Coefficients

Longitudinal Static Stability



Dutch Roll Response Mode



Longitudinal derivatives

$$X_u = -0.058469 \quad C_{x_u} = -0.0080812$$

$$X_w = 0.39695 \quad C_{x_a} = 0.054865$$

$$Z_u = -1.796 \quad C_{z_u} = -3.5774e-05$$

$$Z_w = -28.084 \quad C_{L_a} = 3.8817$$

$$Z_q = -5.264 \quad C_{L_q} = 4.9336$$

Mu= 1.5796e-06 Cmu= 7.402e-07

Mw= -1.4881 Cma= -0.69734

Mq= -0.64741 Cm_q= -2.0573

Neutral Point position= 9.33605in

Lateral derivatives

Y_v= -1.0026 CY_b= -0.13858

Y_p= -0.55368 CY_p= -0.12554

Y_r= 0.3052 CY_r= 0.069199

L_v= -0.26623 Cl_b= -0.030182

L_p= -2.3449 Cl_p= -0.43608

L_r= 0.031573 Cl_r= 0.0058716

N_v= 0.30648 Cn_b= 0.034744

N_p= 0.20424 Cn_p= 0.037982

N_r= -0.093054 Cn_r= -0.017305

_____State matrices_____

Longitudinal state matrix

-0.0184144	0.125019	0	-9.81
-0.565658	-8.84509	33.0324	0
1.54217e-05	-14.5286	-6.32093	0
0	0	1	0

Lateral state matrix

-0.315769	-0.174378	-34.5941	9.81
-3.35971	-29.4683	0.401243	0
2.71954	1.91955	-0.823282	0
0	1	0	0

___Longitudinal modes___

Eigenvalue: -7.585+ -21.87i | -7.585+ 21.87i | -0.007495+ -0.3878i | -
0.007495+ 0.3878i

Eigenvector: 1+ 0i | 1+ 0i | 1+ 0i | 1+ 0i
 113.4+ 71.98i | 113.4+ -71.98i | -0.006671+0.0003364i | -0.006671+-
0.0003364i
 52+ -72.34i | 52+ 72.34i | 0.01534+0.0001683i | 0.01534+-
0.0001683i
 2.217+ 3.147i | 2.217+ -3.147i | -0.001198+ 0.03954i | -0.001198+ -
0.03954i

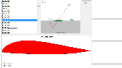
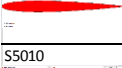
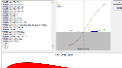
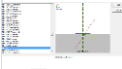
___Lateral modes___

Eigenvalue: -29.3+ 0i | -0.6487+ -9.376i | -0.6487+ 9.376i | -0.006347+
0i

Eigenvector: 1+ 0i | 1+ 0i | 1+ 0i | 1+ 0i
 -17.72+ 0i | -0.1064+ -0.03088i | -0.1064+ 0.03088i | -0.07097+
0i
 1.099+ 0i | 0.01131+ 0.2681i | 0.01131+ -0.2681i | 3.162+
0i
 0.6046+ 0i | 0.004059+ -0.01106i | 0.004059+ 0.01106i | 11.18+
0i

Appendix C: Wingtip Data from RealFlight 6.5

Airfoil	SLOW SPEED BASELINE										PER Battery							
	Downwash (degrees)	"Slow Speed" (MPH)	Altitude (ft)	Thrust Req (lbf)	Battery Rate (sec/ma*hr)	Weight (lb)	Wing Loading (oz/ft^2)	Density (kg/m^3)	Dynamic Visc. (Pa*s)	Wing Area (ft^2)	Flight Time (min)	Range (mi)	C_D,max (-)	C_D,Lift (-)	C_D,Form (-)	C_L (-)	C_L/C_D (-)	
Baseline (E344)	4	35	7150	0.798	0.5	7.021	29.273	0.9885	1.74*10^-5	3.84	33.33	19.44	0.082	0.037	0.045	0.724	8.829268	
NACA0009	6	35	6985	0.648	0.74	7.021	29.273	0.9935	1.74*10^-5	3.84	49.33	28.78	0.066	0.036	0.030	0.720	10.83488	
	5	35	6740	0.65	0.72	7.021	29.273	1.001	1.74*10^-5	3.84	48.00	28.00	0.066	0.036	0.030	0.714	10.80154	
	4	35	7300	0.666	0.73	7.021	29.273	0.9839	1.74*10^-5	3.84	48.67	28.39	0.069	0.037	0.032	0.727	10.54204	
	3																	
	2	35	7070	0.745	0.55	7.021	29.273	0.9909	1.74*10^-5	3.84	36.67	21.39	0.077	0.037	0.040	0.722	9.424161	
S5010	6	35	6830	0.668	0.7	7.021	29.273	0.9982	1.74*10^-5	3.84	46.67	27.22	0.068	0.036	0.032	0.716	10.51048	
	4	35	6940	0.617	0.79	7.021	29.273	0.9982	1.74*10^-5	3.84	52.67	30.72	0.063	0.036	0.027	0.716	11.37925	
	2	35	7030	0.709	0.65	7.021	29.273	0.9921	1.74*10^-5	3.84	43.33	25.28	0.073	0.037	0.036	0.721	9.90268	
MH78	6	35	7310	0.716	0.63	7.021	29.273	0.9830	1.74*10^-5	3.84	42.00	24.50	0.074	0.037	0.037	0.728	9.805866	
	4	35	7150	0.667	0.7	7.021	29.273	0.9882	1.74*10^-5	3.84	46.67	27.22	0.069	0.037	0.032	0.724	10.52624	
	2	35	7230	0.728	0.59	7.021	29.273	0.9856	1.74*10^-5	3.84	39.33	22.94	0.075	0.037	0.038	0.726	9.644231	
NACA M10	6	35	6950	0.747	0.6	7.021	29.273	0.9948	1.74*10^-5	3.84	40.00	23.33	0.076	0.036	0.040	0.719	9.398929	
	4	35	7030	0.655	0.72	7.021	29.273	0.9921	1.74*10^-5	3.84	48.00	28.00	0.067	0.037	0.031	0.721	10.71908	
	2	35	7040	0.791	0.54	7.021	29.273	0.9918	1.74*10^-5	3.84	36.00	21.00	0.081	0.037	0.045	0.721	8.876106	
M49	6	35	6960	0.594	0.83	7.021	29.273	0.9944	1.74*10^-5	3.84	55.33	32.28	0.061	0.036	0.024	0.719	11.81987	
	4	35	6860	0.621	0.8	7.021	29.273	0.9977	1.74*10^-5	3.84	53.33	31.11	0.063	0.036	0.027	0.717	11.30596	
	2	35	6870	0.563	0.9	7.021	29.273	0.9974	1.74*10^-5	3.84	60.00	35.00	0.058	0.036	0.021	0.717	12.47069	
MH 110						7.021	29.273	1.2223	1.74*10^-7	5.84								
						7.021	29.273	1.2223	1.74*10^-8	6.84								
	6	35	7500	0.649	0.77	7.021	29.273	0.9768	1.74*10^-5	3.84	51.33	29.94	0.068	0.038	0.030	0.732	10.81818	
	4	35	7160	0.685	0.68	7.021	29.273	0.9879	1.74*10^-5	3.84	45.33	26.44	0.071	0.037	0.034	0.724	10.24964	
	2	35	7120	0.624	0.78	7.021	29.273	0.9892	1.74*10^-5	3.84	52.00	30.33	0.064	0.037	0.027	0.723	11.2516	
2 -> -2	35	7400	0.642	0.78	7.021	29.273	0.9800	1.74*10^-6	4.84	52.00	30.33	0.067	0.037	0.029	0.730	10.93614		
ESA 40	6	35	6680	0.648	0.73	7.021	29.273	1.0036	1.74*10^-5	3.84	48.67	28.39	0.066	0.036	0.030	0.713	10.83488	
	4	35	7340	0.63	0.77	7.021	29.273	0.9820	1.74*10^-5	3.84	51.33	29.94	0.065	0.037	0.028	0.728	11.14444	
	2	35	7200	0.667	0.7	7.021	29.273	0.9866	1.74*10^-5	3.84	46.67	27.22	0.069	0.037	0.032	0.725	10.52624	
MH 64	6	35	6990	0.579	0.7	7.021	29.273	0.9935	1.74*10^-5	3.84	46.67	27.22	0.059	0.036	0.023	0.720	12.12608	
	4	35	6700	0.554	0.72	7.021	29.273	1.0030	1.74*10^-5	3.84	48.00	28.00	0.056	0.036	0.020	0.713	12.67329	
	2	35	6850	0.554	0.76	7.021	29.273	0.9980	1.74*10^-5	3.84	50.67	29.56	0.057	0.036	0.020	0.717	12.67329	
MH 45	6	35	6710	0.553	0.75	7.021	29.273	1.0026	1.74*10^-5	3.84	50.00	29.17	0.056	0.036	0.020	0.713	12.6962	
	4	35	6825	0.554	0.77	7.021	29.273	0.9989	1.74*10^-5	3.84	51.33	29.94	0.056	0.036	0.020	0.716	12.67329	
	2	35	6720	0.554	0.72	7.021	29.273	1.0023	1.74*10^-5	3.84	48.00	28.00	0.056	0.036	0.020	0.714	12.67329	

	Zero Trim (MAX EFFICIENCY)													C_L/C_D (-)	NonDim Range (-)
	Airspeed (MPH)	Altitude (ft)	Thrust Req (lbf)	Battery Rate (sec/mA*hr)	Density (kg/m^3)	Dynamic Visc. (Pa*s)	Flight Time (min)	Range (mi)	C_D,max (-)	C_D,Lift (-)	C_D,Form (-)	C_L (-)			
	Baseline (E344)														
	49	8050	0.808	0.6	0.9587	1.74*10^-5	40.00	32.67	0.044	0.010	0.034	0.381	8.689356	4.06	
	55	7745	0.923	0.5	0.9687	1.74*10^-5	33.33	30.56	0.039	0.006	0.033	0.299	7.606717	3.95	
	58	7670	1.036	0.41	0.9712	1.74*10^-5	27.33	26.42	0.040	0.005	0.035	0.268	6.777027	3.44	
	73	6500		0.25			36.7	21.4	0.077	0.037	0.04	0.722	9.376623	3.29	
	56	7120	0.933	0.47	0.9892	1.74*10^-5	31.33	29.24	0.038	0.006	0.032	0.282	7.525188	4.11	
	68	7130	1.301	0.29	0.9889	1.74*10^-5	19.33	21.91	0.036	0.003	0.033	0.192	5.396618	3.07	
	97	6690	2.2	0.1	1.0033	1.74*10^-5	6.67	10.78	0.029	0.001	0.028	0.093	3.191364	1.61	
	45	7410	0.605	0.575	0.9797	1.74*10^-5	38.33	28.75	0.038	0.014	0.024	0.442	11.60496	3.88	
	51	7530	0.986	0.42	0.9758	1.74*10^-5	28.00	23.80	0.048	0.008	0.040	0.345	7.12069	3.16	
	61	7270	1.15	0.34	0.9843	1.74*10^-5	22.67	23.04	0.039	0.004	0.035	0.239	6.105217	3.17	
	72	7100	1.45	0.22	0.9899	1.74*10^-5	14.67	17.60	0.035	0.002	0.033	0.171	4.842069	2.48	
	97	6770	2.29	0.1	1.0007	1.74*10^-5	6.67	10.78	0.030	0.001	0.030	0.093	3.065939	1.59	
	97	7110	2.36	0.1	0.9895	1.74*10^-5	6.67	10.78	0.032	0.001	0.031	0.094	2.975	1.52	
	38	6985	0.622	0.8	0.9936	1.74*10^-5	53.33	33.78	0.054	0.026	0.028	0.611	11.28778	4.84	
	41	7350	0.621	0.83	0.9817	1.74*10^-5	55.33	37.81	0.047	0.020	0.027	0.531	11.30596	5.14	
	45	7020	0.683	0.75	0.9925	1.74*10^-5	50.00	37.50	0.042	0.013	0.029	0.436	10.27965	5.34	
	42	7560	0.8	0.55	0.9748	1.74*10^-5	36.67	25.67	0.058	0.018	0.040	0.510	8.77625	3.40	
	45	7370	0.685	0.75	0.9810	1.74*10^-5	50.00	37.50	0.043	0.014	0.029	0.441	10.24964	5.09	
	53	7370	0.811	0.61	0.9810	1.74*10^-5	40.67	35.92	0.037	0.007	0.030	0.318	8.657213	4.87	
	53	7170	0.83	0.6	0.9876	1.74*10^-5	40.00	35.33	0.037	0.007	0.030	0.316	8.459036	4.93	
	38	7460	0.617	0.86	0.9781	1.74*10^-5	57.33	36.31	0.055	0.027	0.027	0.620	11.37925	4.87	
	42	7520	0.652	0.8	0.9761	1.74*10^-5	53.33	37.33	0.047	0.018	0.029	0.509	10.7684	4.96	
	47	7160	0.708	0.73	0.9879	1.74*10^-5	48.67	38.12	0.040	0.011	0.029	0.401	9.916667	5.32	
	57	7050	0.818	0.47	0.9915	1.74*10^-5	31.33	29.77	0.032	0.005	0.026	0.272	8.58313	4.22	
	74	6742	1.231	0.28	1.0016	1.74*10^-5	18.67	23.02	0.028	0.002	0.026	0.160	5.703493	3.41	
	144	6500	4	0.03	1.0095	1.74*10^-5	2.00	4.80	0.024	0.000	0.024	0.042	1.75525	0.74	
	53	6800	0.737	0.55	0.9997	1.74*10^-5	36.67	32.39	0.033	0.007	0.026	0.312	9.526459	4.76	
	67	6800	1.051	0.33	0.9997	1.74*10^-5	22.00	24.57	0.029	0.003	0.027	0.195	6.680304	3.61	
	108	7150	2.33	0.09	0.9882	1.74*10^-5	6.00	10.80	0.025	0.000	0.025	0.076	3.013305	1.51	

	Airspeed	Altitude	Thrust Req	Angle of Trim	Battery Rate	Power Out	Flight Time (min)	Range (mi)	C_D,max (-)	C_D,Lift (-)	C_D,Form (-)	C_L (-)	C_L/C_D (-)
MH 49	25	6715	1.279	18.1	0.21	207.6	14.00	5.83	0.255	0.138	0.117	1.399	5.49
CG 7.55"	30	6715	0.543	3.4	0.75	59.9	50.00	25.00	0.075	0.066	0.009	0.971	12.94
	35	6715	0.495	0.1	0.89	50	59.33	34.61	0.050	0.036	0.014	0.714	14.19
	40	6715	0.538	-1.8	0.84	54.6	56.00	37.33	0.042	0.021	0.021	0.546	13.06
	47	6720	0.683	-3.4	0.6	73.8	40.00	31.33	0.038	0.011	0.027	0.396	10.28
	59	6700	1.005	-5	0.36	127	24.00	23.60	0.036	0.004	0.031	0.251	6.99
	68	6700	1.25	-5.7	0.24	178	16.00	18.13	0.034	0.003	0.031	0.189	5.62
	72	6720	1.397	-5.9	0.21	212	14.00	16.80	0.034	0.002	0.032	0.169	5.03
MH 110	25	6720	0.606	8.5	0.6	72.5	40.00	16.67	0.121	0.138	-0.017	1.399	11.59
	31	6710	0.482	4.1	0.84	53.37	56.00	28.93	0.062	0.058	0.004	0.910	14.57
	36	6705	0.505	1	0.87	51.5	58.00	34.80	0.048	0.032	0.016	0.674	13.91
	38	6720	0.495	0.1	0.89	50.8	59.33	37.58	0.043	0.026	0.017	0.606	14.19
	46	6715	0.648	-2	0.65	69.9	43.33	33.22	0.038	0.012	0.026	0.413	10.84
	63	6700	1.074	-3.6	0.3	140.6	20.00	21.00	0.034	0.003	0.030	0.220	6.54
	103	6730	2.526	-4.9	0.08	490	5.33	9.16	0.030	0.000	0.029	0.082	2.78
MH 110	25	6724	0.73	15.7	0.42	95.8	28.00	11.67	0.145	0.138	0.008	1.399	9.62
.5" forward	30	6715	0.573	8.5	0.69	65.8	46.00	23.00	0.079	0.066	0.013	0.971	12.26
	35	6710	0.521	4.9	0.8	55.65	53.33	31.11	0.053	0.036	0.017	0.714	13.48
	41	6710	0.533	1.7	0.83	53.7	55.33	37.81	0.039	0.019	0.020	0.520	13.18
	46	6711	0.608	0.1	0.72	63.3	48.00	36.80	0.036	0.012	0.024	0.413	11.55
	58	6712	0.852	-1.8	0.44	100.9	29.33	28.36	0.032	0.005	0.027	0.260	8.24
	76	6695	1.419	-3.5	0.2	212.3	13.33	16.89	0.031	0.002	0.029	0.151	4.95
MH 110	24	6700	0.714	5.6	0.5	93	33.33	13.33	0.154	0.162	-0.008	1.517	9.84
.5" aft	31	6706	0.461	0.1	0.98	46.6	65.33	33.76	0.060	0.058	0.001	0.910	15.24
	42	6742	0.582	-3.2	0.74	60.4	49.33	34.53	0.041	0.017	0.024	0.496	12.07
	99	6692	2.4	-5.3	0.07	486	4.67	7.70	0.030	0.001	0.030	0.089	2.93
MH49	25	6750	1.059	14.1	0.25	166	16.67	6.94	0.211	0.138	0.073	1.401	6.63
4 all wing	29	6750	0.482	3.4	0.9	52	60.00	29.00	0.071	0.076	-0.005	1.041	14.57
	33	6758	0.482	0	0.925	47.85	61.67	33.92	0.055	0.045	0.010	0.804	14.57
	55	6747	0.841	-5.3	0.44	100.8	29.33	26.89	0.035	0.006	0.029	0.289	8.35
MH49	25	6725	1.142	18	0.23	189	15.33	6.39	0.228	0.138	0.090	1.399	6.15
4 half wing	35	6765	0.482	1.1	0.95	48.6	63.33	36.94	0.049	0.036	0.013	0.715	14.57
	37	6758	0.459	0	1	46.6	66.67	41.11	0.042	0.029	0.013	0.640	15.30
	43	6756	0.529	-2	0.88	51.3	58.67	42.04	0.036	0.016	0.020	0.474	13.28
	77	6750	1.539	-5.3	0.18	247.5	12.00	15.40	0.032	0.002	0.031	0.148	4.56
	104	6920	2.6	-6	0.07	560	4.67	8.09	0.030	0.000	0.030	0.081	2.70
MH49	25	6760	0.684	10.5	0.54	84	36.00	15.00	0.136	0.138	-0.002	1.401	10.27
4 1/4 wing	31	6760	0.553	4.9	0.716	63	47.73	24.66	0.072	0.058	0.013	0.911	12.70
	40	6740	0.504	0	0.9	50.1	60.00	40.00	0.039	0.021	0.018	0.547	13.94
	51	6750	0.681	-2	0.63	74	42.00	35.70	0.033	0.008	0.025	0.337	10.31
	65	6760	1.17	-3.4	0.27	157	18.00	19.50	0.035	0.003	0.031	0.207	6.00
MILEY	25	6785	0.791	13.3	0.4	110	26.67	11.11	0.158	0.138	0.020	1.402	8.88
7.55 CG	30	6760	0.504	3.4	0.82	53.8	54.67	27.33	0.070	0.067	0.003	0.973	13.94
MH 49	35	6750	0.457	0	1	45.3	66.67	38.89	0.046	0.036	0.011	0.715	15.37
	44	6750	0.629	-3.4	0.66	67.7	44.00	32.27	0.040	0.014	0.026	0.452	11.17
	64	6760	1.14	-6	0.275	157.5	18.33	19.56	0.035	0.003	0.031	0.214	6.16
Half Elev	26	6725	0.605	12.5		72.3							
	31	6705	0.519	6.4		56.4							
	40	6740	0.546	0		55.6							
	47	6710	0.634	-2		64.66							
	95	6815	2.027	-6		375							
Half Elev, 50%	25	6730	0.627	11.8		75.2							
	35	6726	0.485	2.6		51.7							
	41	6730	0.526	0		52.8							
	91	6714	2.014	-5.1		348							
	129	6750	3.7	-5.8		884							